Australian Journal of Basic and Applied Sciences, 10(14) September 2016, Pages: 299-306

AUSTRALIAN JOURNAL OF BASIC AND APPLIED SCIENCES

ISSN:1991-8178 EISSN: 2309-8414
Journal home page: www.ajbasweb.com

Inverse Current Measurement Method for Parameters Estimating of Miniature Loudspeaker

[1]Chi-Chang Wang, [2]Jin-Huang Huang, [3]Thi-Thao Ngo, [4]Van-The Than

[1]Department of Mechanical and Computer-Aided Engineering, Feng Chia University, No. 100 Wenhwa Rd., Seatwen, Taichung, Taiwan 40724, R.O.C.
[2]Department of Mechanical and Computer-Aided Engineering, and Electroacoustic Graduate Program, Feng Chia University, No. 100 Wenhwa Rd., Seatwen, Taichung, Taiwan 40724, R.O.C.
[3]Faculty of Mechanical Engineering, Hung Yen University of Technology and Education, Khoai Chau, Hung Yen, Vietnam.
[4]Ph. D. Program of Mechanical and Aeronautical Engineering, Feng Chia University, No. 100 Wenhwa Rd., Seatwen, Taichung, Taiwan 40724, R.O.C.

Address For Correspondence:
Van-The Than, Ph. D. program of Mechanical and Aeronautical Engineering, Feng Chia University, No. 100 Wenhwa Rd., Seatwen, Taichung, Taiwan 40724, R.O.C.
E-mail: thanthe.ck@gmail.com; thanthe.ck@mail.fcu.edu.tw

ARTICLE INFO

Article history:
Received 18 July 2016
Accepted 21 August 2016
Published 3 September 2016

Keywords:
Inverse method
Miniature loudspeaker
Scale factor
Measurement error

ABSTRACT

This paper presents an inverse method to accurately estimate five electroacoustic parameters of miniature loudspeaker, which are voice-coil inductance L_e, mechanical mass M_m, mechanical resistance R_m, mechanical stiffness K_m and force factor Bl, based on only measured current. Transduction equations of the loudspeaker are expressed for the inverse computation procedure. Results show that the estimated currents as well as the five parameters are agreement with exact values even measurement errors are involved. In addition, effects of scale factors and optimization methodology are also analyzed. It believes that the method has potential to predict electroacoustic parameters of the miniature loudspeaker which are usually difficult to directly measure.

INTRODUCTION

Miniature loudspeaker (ML) in Fig. 1 is widely used in acoustic technology. Microphone sound reception and laser displacement measurement methods were used to measure electroacoustic lumped parameters. The traditional measurement principle changes the loudspeaker impedance frequency response curve peak frequency and determines the parameter values according to the change, such as close-box method (Beranek 1993 and David 1978) and add mass method (Remeberto 1991). In recent years, laser measurement technology (Klippel, 1990, 1999) and system identification (Knudsen *et al.*, 2007) to measure the voice coil displacement and some parameters in Z-domain are become popular. However, the present ML diaphragm is too light, and the voice coil stroke is too short. Clay around the light diaphragm may cause nonlinear vibration characteristics of the support suspension system of loudspeaker (Pedersen & Agerkvist, 2007; Pawar *et al.*, 2012; Chun Chang *et al.*, 2012). In addition, the ML diaphragm can be made by PE or PVC transparent material instead of traditional paper or rubber. Therefore, the previous laser method based on displacement may not be appropriated for measuring parameters on the kind of ML. Fortunately, lumped parameter model based on differential equation form to analyze loudspeaker has been proposed by Klippel (Klippel, 1990, 1999) and Beranek (Beranek, 1993). As shown in Fig. 2, the lumped parameter model of ML includes parameters of voice-coil inductance L_e, voice-

To Cite This Article: Chi-Chang Wang, Jin-Huang Huang, Thi-Thao Ngo, Van-The Than., Inverse Current Measurement Method for Parameters Estimating of Miniature Loudspeaker. ***Aust. J. Basic & Appl. Sci.**, 10(14): 299-306, 2016*

Australian Journal of Basic and Applied Sciences, 10(14) September 2016, Pages: 299-306

coil resistance R_e, mechanical mass M_m, mechanical resistance R_m, mechanical stiffness K_m, and force factor Bl; and it is divided into electrical and mechanical domains. These five parameters are normally given as input values for solving differential equations to obtain displacement $X(t)$ and current $I(t)$ of ML. Appling inverse method to estimate the five parameters based on the differential equation of the lumped parameter model of ML has never presented in any previous researches. In this study, the inverse method, which has been successfully applied for solving heat transfer problems (Wang, 2011; Lin David *et al.*, 2008; Chen & Su, 2008), is used to estimate the five parameters by using measured current values. Influence of parameter scales, optimization method, and measurement errors on inverse results are carried out and discussed.

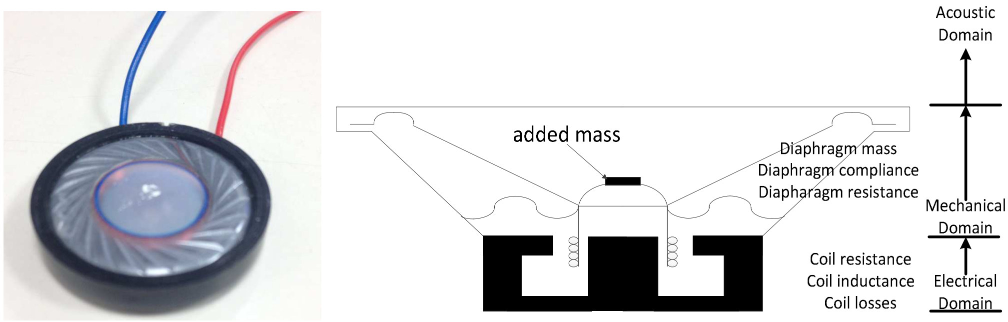

(a) Real ML. (b) Schematic representation.

Fig. 1: Miniature loudspeaker

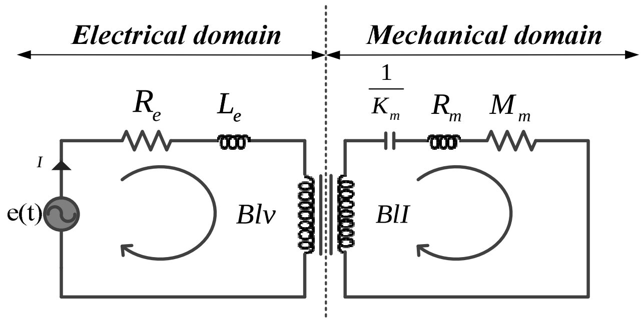

Fig. 2: The equivalent circuit of the ML

2. Inverse Current Measurement Method:

2.1. Lumped parameter model:

According to the structure of ML in Fig. 1, an equivalent circuit for ML is established and shown in Fig. 2. Wavelength generated in low-frequency vibration of ML is quite larger than the ML's geometry. Therefore, the components in electrical domain, mechanical domain and acoustic domain can be regarded as lumped parameter model. As observed, the electrical domain contains two parameters (R_e and L_e) and three parameters (M_m , R_m and K_m) in the mechanical domain. Two domains are connected through the force factor Bl . Therefore, the governing equation of the ML can be deduced from the lumped parameter model by using Newton laws of motion and Kirchhoff's voltage law as:

$$M_m \frac{d^2X(t)}{dt^2} + R_m \frac{dX(t)}{dt} + K_m X(t) = Bl\ I(t) \tag{1}$$

$$L_e \frac{dI(t)}{dt} + R_e I(t) + Bl \frac{dX(t)}{dt} = e(t) \tag{2}$$

where $e(t)$ is the time-dependent input voltage of the ML. $I(t)$ and $X(t)$ are the voice coil current and diaphragm displacement, respectively.

2.2. Objective function and optimization method:

The inverse problem is concerned with estimating electroacoustic parameters based on knowledge of the current in ML. Unknown vector can be expressed as:

$$\vec{\mathbf{w}} = [M_m\ R_m\ K_m\ Bl\ L_e] \tag{3}$$

Then an objective function J is defined by measured value $\mathrm{I}_{mea}(t)$ and estimated value $\mathrm{I}(t)$ as

$$J(\vec{\mathbf{w}}) = \int_0^{t_f} \left[I(\vec{\mathbf{w}};t) - I_{mea}(t) \right]^2 dt \tag{4}$$

when the objective function J is minimum, the estimated value $I_{inv}(t)$ approaches to the measured value $I_{mea}(t)$. There are many optimal methods to minimize the J value. In present paper, conjugate gradient method (CGM) and steepest descent method (SDM) are employed to find the best direction and search step size. In general, the SDM has fast convergence along the negative gradient at value far from the optimal values, but it requires a long time for convergence when the value are near the optimal values. Whereas the CGM is an algorithm for finding the nearest local minimum of variables which presuppose that the gradient of the function can be computed. For CGM, the iteration equation is given as:

$$\vec{\mathbf{w}}^{(k+1)} = \vec{\mathbf{w}}^{(k)} - \beta^{(k)} \vec{\mathbf{P}}^{(k+1)} \tag{5}$$

$$\vec{\mathbf{P}}^{(k+1)} = \nabla J^{(k)} + \gamma^{(k)} \vec{\mathbf{P}}^{(k)} \tag{6}$$

where k is the number of iterations. $\beta^{(k)}$ stands the search step size. $\vec{\mathbf{P}}^{(k+1)}$ denotes the descent direction. $\gamma^{(k)}$ is conjugate coefficient and can calculate by one of the three forms in Eq. (7).

$$\gamma_{FR}^{(k)} = \frac{\left\| \nabla J^{(k)} \right\|^2}{\left\| \nabla J^{(k-1)} \right\|^2},\ \gamma_{DY}^{(k)} = \frac{\left\| \nabla J^{(k)} \right\|^2}{\left\| \nabla J^{(k-1)} \right\|^2},\ \gamma_{HS}^{(k)} = \frac{\left\| \nabla J^{(k)} \right\|^2}{\left\| \nabla J^{(k-1)} \right\|^2},\ k \ge 1 \tag{7}$$

and $\nabla J^{(k)}$ represents the gradient of the objective function.

$$\nabla J = \left[\frac{\partial J}{\partial M_m}\ \frac{\partial J}{\partial R_m}\ \frac{\partial J}{\partial K_m}\ \frac{\partial J}{\partial Bl}\ \frac{\partial J}{\partial L_e} \right]^T \tag{8}$$

If $k = 0$ then $\gamma^{(k)} = 0$. When the descent direction disregards $\gamma^{(k)} \vec{\mathbf{P}}^{(k)}$, $\vec{\mathbf{P}}$ of Eq. (6) degrades into the gradient of the objective function ∇J, known as SDM. The $I(t)$, ∇J and β must be found through direct, adjoint and sensitivity problem.

2.3. Solving direct problem for $I(t)$:

We use the hybrid spline difference method proposed by Wang (Wang *et al.*, 2012) to solve for determining $I(t)$ because of its simplicity and high accuracy ($O(\Delta t^4)$) compared to the finite difference method ($O(\Delta t^2)$). The following discrete expression to discretize differential equation as

$$I(t^n) = \frac{p^{n-1} + 10p^n + p^{n+1}}{12};\ \frac{dI(t^n)}{dt} = \frac{p^{n+1} - p^{n-1}}{2\Delta t} \tag{9}$$

where p and n are the parameters of spline value and time; then P^{n+1}, the value of $I(t^n)$ and its derivation can be obtained rapidly.

Substituting Eq. (9) into Eqs. (1-2), we have:

$$M_m \frac{p_i^{n-1} - 2p_i^n + p_i^{n+1}}{\Delta t^2} + R_m \left[\frac{p_i^{n+1} - p_i^{n-1}}{2\Delta t} - \Delta \dot{f}^n \right] + K_m \frac{p_i^{n-1} + 10p_i^n + p_i^{n+1}}{12} = Bl \left(\frac{p_i^{n-1} + 10p_i^n + p_i^{n+1}}{12} \right) \tag{10}$$

$$L_e \left(\frac{p_x^{n+1} - p_x^{n-1}}{2\Delta t} - \Delta i^n \right) + R_e \left(\frac{p_x^{n-1} + 10p_x^n + p_x^{n+1}}{12} \right) + Bl \left[\frac{p_x^{n+1} - p_x^{n-1}}{2\Delta t} - \Delta \dot{X}^n \right] = e(t) \tag{11}$$

With given value of vector $\vec{\mathbf{w}} = [M_m\ R_m\ K_m\ Bl\ L_e]$, the current values $I(t^n)$ can be obtained.

2.4. Adjoint problem for ∇J :

To determine the gradient of the object function ∇J in Eq. (8), solving an adjoint problem is applied in this study. Eqs. (1) and (2) are multiplied by the Lagrange multipliers $\lambda(t)$ and $G(t)$, respectively. The object function now becomes:

$$\begin{aligned}J(\vec{\mathbf{w}};\lambda;G) &= Eq.\,(4)+\int_0^{t_f}\lambda(t)Eq.\,(1)dt+\int_0^{t_f}G(t)Eq.\,(2)dt\\ &=\int_0^{t_f}[I(t)-I_{mea}(t)]^2\,dt+\int_0^{t_f}\lambda(t)\left[M_m\frac{d^2X(t)}{dt^2}+R_m\frac{dX(t)}{dt}+K_mX(t)-BlI(t)\right]dt\\ &+\int_0^{t_f}G(t)\left[L_e\frac{dI(t)}{dt}+\mathrm{R_e}\,I(t)+Bl\frac{dX(t)}{dt}-e(t)\right]dt\end{aligned} \tag{12}$$

The unknown $\vec{\mathbf{w}}$ is added a perturbing, $\delta\vec{\mathbf{w}}=[\delta M_m\ \delta R_m\ \delta K_m\ \delta Bl\ \delta L_e]$, and then replaced to Eq. (12), it yields:

$$\begin{aligned}\delta J(\vec{\mathbf{w}};\lambda;G) &= \left[R_m\lambda(t)\delta X(t)+L_eG(t)\delta I(t)+BlG(t)\delta X(t)\right]\Big|_0^{t_f}\\ &+\left[M_m\lambda(t)\frac{d\delta X(t)}{dt}+M_m\frac{d\lambda(t)}{dt}\delta X(t)\right]\Bigg|_0^{t_f}\\ &+\int_0^{t_f}\left[M_m\frac{d^2\lambda(t)}{dt^2}-R_m\frac{d\lambda(t)}{dt}+K_m\lambda(t)-Bl\frac{dG(t)}{dt}\right]\delta X(t)dt\\ &+\int_0^{t_f}\left[-L_e\frac{dG(t)}{dt}-Bl\lambda(t)+2[I(t)-I_{mea}(t)]\right]\delta I(t)dt\\ &+\int_0^{t_f}\lambda(t)\left(\frac{d^2X(t)}{dt^2}\delta M_m+\frac{dX(t)}{dt}\delta R_m+X(t)\delta K_m-I(t)\delta Bl\right)dt\\ &+\int_0^{t_f}G(t)\left(\frac{dI(t)}{dt}\delta L_e+I(t)\delta\mathrm{R_e}+\frac{dX(t)}{dt}\delta Bl\right)dt\end{aligned} \tag{13}$$

As $I(0)$ and $dX(0)/dt$ are given, $\delta I(0)$ and $d\delta X(0)/dt$ are zero. In addition, the micro variable $\delta I(t)$ is not zero, and the optimal solution occurs when the $\delta J(\vec{\mathbf{w}};\lambda;G)$ of the above equation is zero, the adjoint equation can be obtained

$$\begin{aligned}&M_m\frac{d^2\lambda(t)}{dt^2}-R_m\frac{d\lambda(t)}{dt}+K_m\lambda(t)=Bl\frac{dG(t)}{dt}\\ &-L_e\frac{dG(t)}{dt}=Bl\lambda(t)-2[I(t)-I_{mea}(t)]\end{aligned}\quad ,t\in(t_f,0) \tag{14}$$

The accompanied final value conditions are

$$G(t_f)=0,\ \lambda(t_f)=0\ and\ d\lambda(t_f)/dt=0 \tag{15}$$

According to literature (Lasdon *et al.*, 1967), we can write as:

$$\delta J(\vec{\mathbf{w}})=\int_0^{t_f}\delta\vec{\mathbf{w}}\nabla Jdt=\int_0^{t_f}\left(\delta M_m\frac{\partial J}{\partial M_m}+\delta R_m\frac{\partial J}{\partial R_m}+\delta K_m\frac{\partial J}{\partial K_m}+\delta Bl\frac{\partial J}{\partial Bl}+\delta L_e\frac{\partial J}{\partial L_e}\right)dt \tag{16}$$

Compare Eq. (16) with the integral term of the last two terms on the right of Eq. (13), the gradient of objective function is established as:

$$\begin{aligned}\nabla J &= \begin{bmatrix}\frac{\partial J}{\partial M_m} & \frac{\partial J}{\partial R_m} & \frac{\partial J}{\partial K_m} & \frac{\partial J}{\partial Bl} & \frac{\partial J}{\partial L_e}\end{bmatrix}^T\\ &=\left[\int_0^{t_f}\lambda(t)\frac{d^2X(t)}{dt^2}dt,\int_0^{t_f}\lambda(x)\frac{dX(t)}{dt}dt,\int_0^{t_f}\lambda(t)X(t)dt,\int_0^{t_f}\left(G(t)\frac{dX(t)}{dt}-\lambda(t)I(t)\right)dt,\int_0^{t_f}G(t)\frac{dI(t)}{dt}dt\right]^T\end{aligned} \tag{17}$$

When the gradient of objective function ∇J is obtained, $\vec{\mathbf{P}}$ and γ can be acquired by Eqs. (6) and (7), respectively.

2.5 Sensitivity problem for β :

The search step size, β, is defined as

$$\beta=\frac{\int_0^{t_f}[I(t)-I_{mea}(t)]\delta I(t)dt}{\int_0^{t_f}\delta I^2(t)dt} \tag{18}$$

For the micro variable $\delta I(t)$ of $I(t)$, we must solve the sensitivity problem as

$$M_m\frac{d^2\delta X(t)}{dt^2}+R_m\frac{d\delta X(t)}{dt}+K_m\delta X(t)=-\frac{d^2X(t)}{dt^2}\delta M_m-\frac{dX(t)}{dt}\delta R_m-X(t)\delta K_m+I(t)\delta Bl+Bl\delta I(t) \tag{19}$$

$$L_e \frac{d\delta I(t)}{dt} = -\frac{dI(t)}{dt}\delta L_e - \frac{dX(t)}{dt}\delta Bl - Bl\frac{d\delta X(t)}{dt} \quad (20)$$

with initial conditions:

$$\delta I(t) = 0 \;\; for \; t = 0; \delta X(t) = 0 \; and \; d\delta X(t)/dt = 0 \;\; for \; t = 0 \quad (21)$$

3. Scale factors:

Because of having large difference between some unknown values, in order to avoid error occurs when calculating value of ∇J, some unknown parameters should be divided by scale factors to get appropriate of these unknown parameters. The unknowns are rewrite as follows:

$$\overline{M_m} = \frac{M_m}{S_{M_m}}; \overline{R_m} = \frac{R_m}{S_{R_m}}; \overline{K_m} = \frac{K_m}{S_{K_m}}; \overline{Bl} = \frac{Bl}{S_{Bl}}; \overline{L_e} = \frac{L_e}{S_{L_e}} \quad (22)$$

where S is the scale factor, $\overline{M_m}, \overline{R_m}, \overline{K_m}, \overline{Bl}$ *and* $\overline{L_e}$ are new predicted parameters.

RESULT AND DISCUSSION

The exact values of $[M_m \quad R_m \quad K_m \quad Bl \quad L_e]$ are listed in Table 1. An input excitation voltage $e(t) = 5\times10^3\sin(2\pi ft)$ is employed to get exact current $I_{mea}(t)$. Thus, the maximum voltage is $5\times10^3 mV$ and the stimulus frequency is $f = 100 + 150\,\mathrm{Sin}(\pi\, t/t_f)$. Total simulation time is $t_f = 3\sec$.

Table 1: Miniature loudspeaker parameters

Parameters	M_m *(kg)*	R_m *(kg/s)*	K_m *(N/m)*	Bl *(N/A)*	L_e *(H)*	R_e *(Ohm)*
Value	9.45E-4	0.113	699.3	1.68	1.1E-4	3.51

4.1. Influence of scale factor:

Fig. 3(a) shows the gradient direction and value when scale factors are not used. It is observed that the gradient value of K_m and L_e are too different. In addition, when the search direction is not parallel with K_m axis due to numerical computation error and the search step cannot move forward under having large distinction between gradient magnitudes of K_m and L_e. Hence, scale factors are employed to treat this problem. The differences of the gradient values are reduced to obtain highest convergence speed (see Fig. 3(b)).

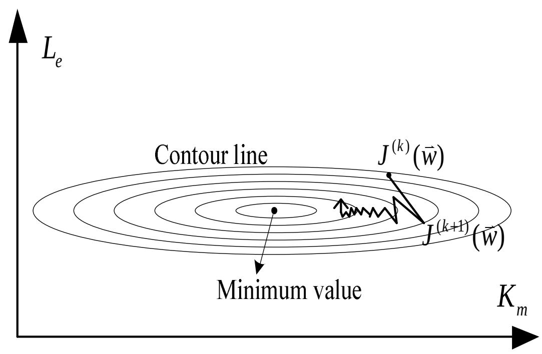

(a) Without scale factors

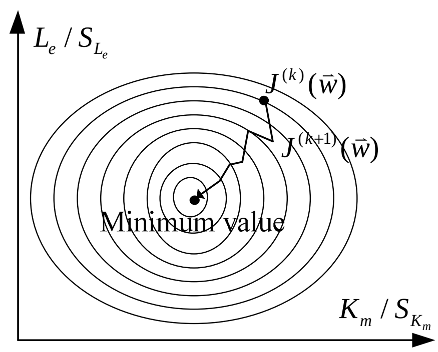

(b) With scale factors

Fig. 3: Schematic diagram of search direction

Some numerical simulation for different scale factors are performed and tabled in Table 2. For case $S_{K_m} = 1E3$ and $S_{L_e} = 1E-4$, if $S_{M_m} > 1E-3$ the objective function $J(\mathbf{w})$ is difficult to reach $1E-10$ after 30 iterations. However, the objective function can be approached to $1E-10$ by using $S_{M_m} < 1E-3$ after maximum 30 iterations. For cases of $S_{K_m} > 1E3$, $S_{L_e} > 1E-4$ and $S_{L_e} < 1E-6$, the objective function cannot also converge to $1E-10$. From Table 2, it evidences that value of S_{M_m} and S_{K_m} should not be greater than $1E-3$ and $1E3$, respectively. While value of S_{L_e} should be from $1E-4$ to $1E-6$. Through all analyses, one can conclude that the choosing appropriate scale factors must be done for situations of exiting large difference between unknowns.

Table 2: Influence of scale factors on number of iterations

S_{M_m} $(S_{K_m}=1E3)$ $(S_{L_e}=1E-4)$	Number		S_{K_m} $(S_{M_m}=1E-3)$ $(S_{L_e}=1E-4)$	Number		S_{L_e} $(S_{M_m}=1E-3)$ $(S_{K_m}=1E3)$	Number
>1E-3	--		1	19		>1E-4	--
1E-3	30		10	19		1E-4	30
1E-4	18		1E2	23		1E-5	41
1E-5	19		1E3	30		1E-6	80
1E-6	19		>1E3	--		<1E-6	--

4.2. Comparison of CGM with SDM:

To compare convergence capability of CGM and SDM, the number of iterations and value of the objective function for these optimal methods are shown in Fig. 4. It evidences that the SDM cannot converge toward a minimum value ($1E-10$) after 50 iterations while the objective function can reach for the CGM. In addition, the convergence capacity for different formula of conjugate coefficients in the CGM are analyzed and compared. The results indicate that used the γ^{HS} formula can get the highest convergence speed. Hence, the CGM with γ^{HS} formula is chosen to optimize the objective function.

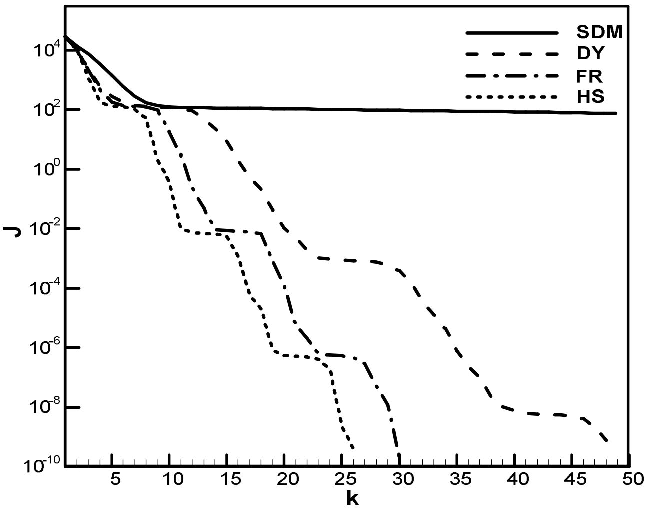

Fig. 4: Comparison of the SDM and CGM (*DY*, *FR* and *HS*)

Table 3: Influence of current measurement error σ on prediction result

σ	The estimate parameters with σ					Average Error (%)
	M_m	R_m	K_m	Bl	L_e	
0	9.45000E-4	0.113000	699.300	1.68000	1.1000E-4	0.000
10	9.47020E-4	0.113308	700.589	1.68123	1.0982E-4	0.236
30	9.57669E-4	0.114143	707.274	1.68982	1.1127E-4	1.251
50	9.59452E-4	0.114863	708.589	1.69026	1.1086E-4	1.509

Exact and inverse current results are figured out in Fig. 5. It can see that the estimated currents agree well with exact values. Moreover, the estimated parameters are much closed to the exact values, as found in Table 3. Thus, the proposed method can correctly predict the ML parameters.

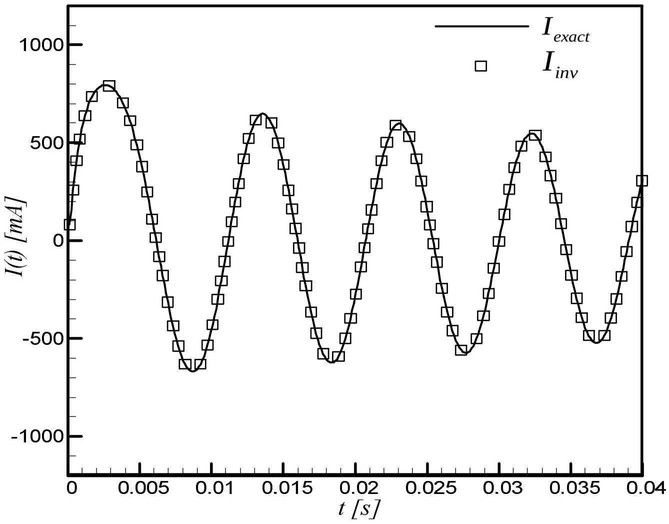

Fig. 5: Comparison of exact and inverse solutions

4.3. Effect of measurement error:

In fact, measurement process always has error degree which may be caused by instrument, equipment, environment and nonlinear distortion of ML. Regarding effects of measurement error on inverse results must be carried out through adding the standard deviations σ into measured data. The measurement error using normal distribution is defined as

$$\varpi = \frac{1}{\sigma\sqrt{2\pi}} \int_{-\infty}^{I_{mea}} e^{-0.5[(t-I_{exact})/\sigma]^2} dt \tag{25}$$

where I_{mea} and I_{exact} are the measured currents with and without measurement errors, respectively. Fig. 6 shows a comparison of the exact solution and inverse results. Clearly, the estimated current is in agreement with measured value, while the measurement error has effects on estimated ML parameters. The estimated $\vec{w}$ for different values of σ is shown in Table 3. It is seen that value of $\vec{w}$ slightly increases with increased measurement errors. The average errors of $\vec{w}$ also rise with augment measurement error. Maximum of the average error is 1.509% when $\sigma = 50mA$. It demonstrates that the proposed inverse method can accurately estimate parameters of ML even measurement errors are involved.

Average error: $\frac{1}{5}\sum_{i=1}^{5}\left|\frac{\vec{w}_i^{exact} - \vec{w}_i^{inv}}{\vec{w}_i^{exact}}\right| \times 100\%$ (26)

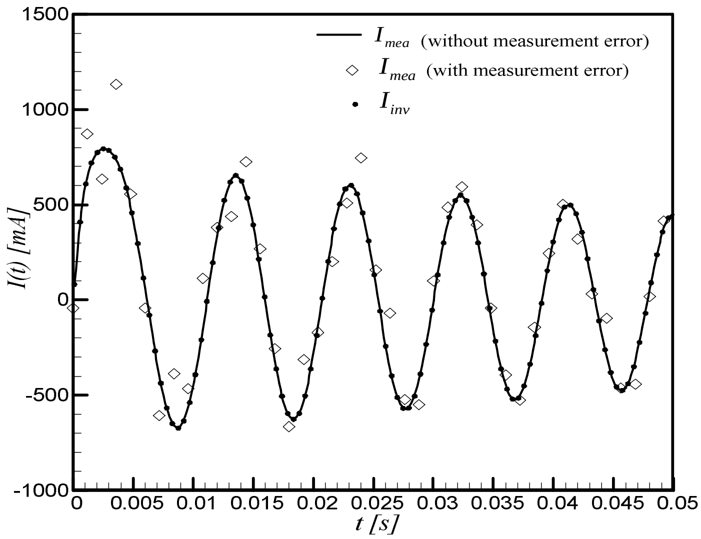

Fig. 6: Inverse results with measurement error

Conclusion:

This paper establishes an inverse method for estimating five parameters of ML based on the measurement current data. The results shown that the inverse solutions are in good agreement with exact solution. The scale factors and optimal algorithms significantly affect the convergence speed and value of objective function. The

Australian Journal of Basic and Applied Sciences, 10(14) September 2016, Pages: 299-306

errors of inverse results slight increase with increasing measurement errors. However, the maximum average errors of estimated results is only 1.509% corresponding to $\sigma = 50mA$. It is believed that the proposed method has potential for predicting parameters in ML and may give useful information to construct high quality ML.

ACKNOWLEDGEMENT

This study is financially sponsored by the National Science Council under Grant No. MOST 103-2221-E-035-030-MY2. The authors also thank Merry Electronic Co. for partial finance and loudspeakers.

REFERENCES

Beranek, L.L., 1993. Acoustics, Melville, New York: American Institute of Physics, pp: 47-90.

David Weems, 1978. How to Design, Build, & Test Complete Speaker Systems, 1st ed., TAB Books.

Remeberto, G.M.,1991. “Measurement of the Thiele-Small Parameters for a given Loudspeaker, Without Using a Box”, Presented at the 91th AES convention, New York.

Klippel, W., 1990. ‘Dynamic Measurement and Interpretation of the Nonlinear Parameters of Electrodynamics Loudspeakers’, Journal of the Audio Engineering Society, 38: 944-955.

Klippel, W., 1999. ‘Measurement of large-signal parameters of electrodynamic transducer’, on the AES E-Library: PN. 5008(E-8), (Presented at the 107th AES convention, Germany, 1999).

Klippel, W., 1999. ‘Measurement of loudspeaker parameters by inverse nonlinear control’, The Journal of the Acoustical Society of America, 105: 1359-1359.

Knudsen, M.H., J.G. Jensen, V. Julskjaer and P. Rubak, 1989. ‘Determination of Loudspeaker Driver Parameters Using a System Identification Technique’, Journal of the Audio Engineering Society, 37: 700-708.

Pedersen, B.R., F.T. Agerkvist, 2007. ‘Time varying behavior of the loudspeaker suspension’, *123th AES convention*, New York, pp: 7192.

Pawar, S.J., Soar Weng, Jin H. Huang, 2012. ‘Total harmonic distortion improvement for elliptical miniature loudspeaker based on suspension stiffness nonlinearity’, IEEE Trans. Consumer Electron., 58(2): 221-227.

Chun Chang, S.J., Pawar, Soar Weng, Y.C. Shiah, Jin H. Huang, 2012. ‘Effect of nonlinear stiffness on the total harmonic distortion and sound pressure level of a circular miniature loudspeaker-experiments and simulations’, IEEE Trans. Consumer Electron., 58(2): 212-220.

Beranek, L.L., 1993. ‘Acoustics’, Melville, New York: American Institute of Physics, pp: 47-90.

Wang, C.C., 2010. ‘Direct and Inverse solutions with non-Fourier effect on the irregular shape’, International Journal of Heat and Mass Transfer, 53: 2685-2693.

Lin David, T.W., W.M. Yan, H.Y. Li, 2008. ‘Inverse problem of unsteady conjugated forced convection in parallel plate channels’ , International Journal of Heat and Mass Transfer, 51: 993-1002.

Chen, C.K. and C.R. Su, 2008. ‘Inverse estimation for temperatures of outer surface and geometry of inner surface of furnace with two layer walls’, Energy Conversion and Management, 49: 301-310.

Wang, C.C., L.P. Chao, W.J. Liao, 2012. ‘Hybrid Spline Difference Method (HSDM) for Transient Heat Conduction’, Numerical Heat Transfer – Part B - Fundamentals, 61(2): 129-146.

Lasdon, L.S., S.K. Mitter and A.D. Warren,1967. ‘The Conjugate Gradient Method for Optimal Control Problem’, IEEE Transactions on Automatic Control, AC-12(2): 132-138.